LBL-38672
UC-427
Preprint

ERNEST ORLANDO LAWRENCE
BERKELEY NATIONAL LABORATORY

The Periodic Table of Vacuum Arc Charge State Distributions

A. Anders
Accelerator and Fusion Research Division

May 1996
Submitted to *Physical Review E*

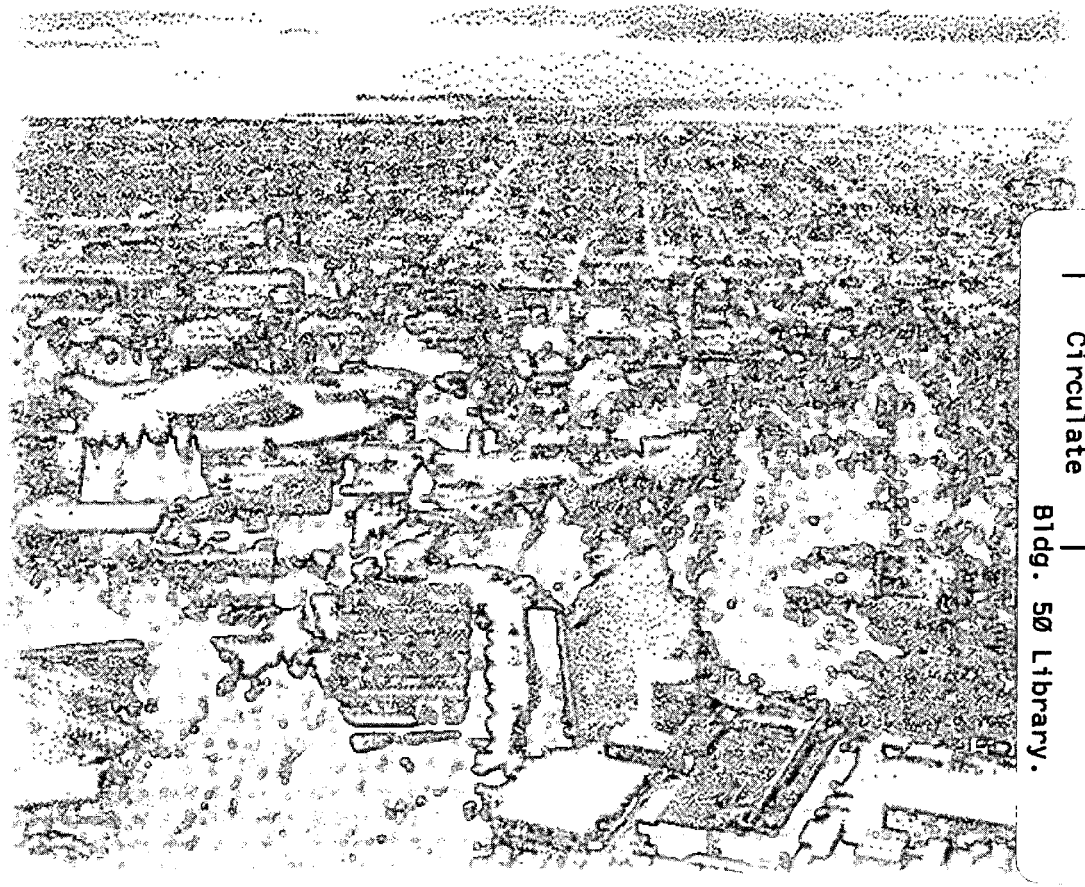

DISCLAIMER

LBL-38672
UC-427

The Periodic Table of Vacuum Arc Charge State Distributions

André Anders

Ernest Orlando Lawrence Berkeley National Laboratory
University of California, Berkeley, California 94720

Phone (510) 486-6745
Fax (510) 486-4374
e-mail aanders@lbl.gov

This preprint contains information which has been submitted for publication in the *Physical Review E.*

May 1996

This work was supported by the U.S. Department of Energy, Division of Advanced Energy Projects, under contract No. DE-AC03-76SF00098.

The Periodic Table of Vacuum Arc Charge State Distributions

André Anders

Ernest Orlando Lawrence Berkeley National Laboratory
University of California, Berkeley, California 94720

ABSTRACT

Ion charge state distributions (CSDs) are experimentally known for 50 elements but theoretical understanding is unsatisfactory. CSDs of vacuum arc plasmas are calculated under the assumption that the spot plasma experiences an instantaneous transition from equilibrium to non-equilibrium while expanding. Observable charge state distributions are the result of a freezing process at this transition. "Frozen" CSDs have been calculated using Saha equations in the Debye-Hückel approximation of the non-ideal plasma for all metals of the Periodic Table, and for carbon, silicon, and germanium. The results are presented in a "Periodic Table of CSDs". The table contains also the mean ion charge state, the neutral vapor fraction, and the effective plasma temperature and density at the freezing point for each element.

I. INTRODUCTION

The electrical current of an arc discharge between solid electrodes in vacuum is transported by the plasma produced by the discharge itself. The plasma usually originates from cathode spots - locations of very small area with very high current density, plasma density, and temperature [1-4]. The observable charge state distribution (CSD) of ions is an important plasma feature which gives insight into the physics of plasma formation. Furthermore, high charge states are of practical interest for vacuum arc ion sources since the ion beam energy is proportional to the ion charge, $E = Q\,U_{extr}$, where U_{extr} is the extractor voltage.

CSDs of ions of low-current plasmas have been extensively studied using time-of-flight charge-to-mass spectrometry [5-14]. It has been found that there exist material-specific CSDs which depend very little on the current (current range 50-300 A, Ref. [12]). Charge state are higher at the beginning of an arc discharge and become constant after about 100 μs [10, 15]. The most complete table of CSD (at arc current 100 A, measured about 100 μs after arc ignition) is given in Ref. [13] for 50 cathode materials, see also Table I. It has been found that the ion charge states can be enhanced by external magnetic fields [10-12, 16] and by high discharge currents [14, 17].

In this paper we discuss the formation of ions in vacuum arc discharges for all metallic elements of the Periodic Table based on the ideas that (i) local thermodynamic equilibrium (LTE) can be assumed in the vicinity of cathode spots [18], (ii) Saha equations of weakly non-ideal plasmas (Debye-Hückel approximation) describe the CSDs correctly as long as LTE is valid, (iii) CSDs remain constant (they "freeze") when the plasmas expand into the vacuum and become non-LTE plasmas, and (iv) the fluctuations of plasma temperature and density at freezing are small enough to allow the introduction of an "effective freezing temperature" and an "effective freezing density" for each element.

Table I. (next page) Elementary cathode materials, their nuclear charge number Z; melting point (°C); boiling point (°C), both from Ref. [30]; mean ion charge state $\overline{Q}$, Ref. [13] and detailed distribution (%, particle fraction), Ref. [13]. Note that the latter data are experimentally obtained by averaging over many individual discharges with arc currents of about 100 A.

Z		T_{melt} (°C)	T_{boil} (°C)	$\overline{Q}$	f_1 (%)	f_2 (%)	f_3 (%)	f_4 (%)	f_5 (%)	f_6 (%)
3	Li	180.5	1347	1.00	100					
6	C	3550	4827	1.00	100					
12	Mg	648.8	1090	1.54	46	54				
13	Al	660.4	2467	1.73	38	51	11			
14	Si	1410	2355	1.39	63	35	2			
20	Ca	839	1484	1.93	8	91	1			
21	Sc	1541	2831	1.79	27	67	6			
22	Ti	1660	3287	2.03	11	75	14			
23	V	1890	3380	2.14	8	71	20	1		
24	Cr	1857	2672	2.09	10	68	21	1		
25	Mn	1244	1962	1.53	49	50	1			
26	Fe	1535	2750	1.82	25	68	7			
27	Co	1495	2870	1.73	34	59	7			
28	Ni	1453	2732	1.76	30	64	6			
29	Cu	1083	2567	2.06	16	63	20	1		
30	Zn	419.6	907.0	1.20	80	20				
32	Ge	937.4	2830	1.40	60	40				
38	Sr	769	1384	1.98	2	98				
39	Y	1522	3338	2.28	5	62	33			
40	Zr	1852	4377	2.58	1	47	45	7		
41	Nb	2468	4742	3.00	1	24	51	22	2	
42	Mo	2617	4612	3.06	2	21	49	25	3	
46	Pd	1552	3140	1.88	23	67	9	1		
47	Ag	1410	2355	2.14	13	61	25	1		
48	Cd	320.9	765	1.32	68	32				
49	In	156.6	2080	1.34	66	34				
50	Sn	232	2270	1.53	47	53				
51	Sb	630.7	1750	1.00	100					
56	Ba	725	1640	2.00	0	100				
57	La	921	3457	2.22	1	76	23			
58	Ce	799	3426	2.11	3	83	14			
59	Pr	931	3512	2.25	3	69	28			
60	Nd	1021	3068	2.17	0	83	17			
62	Sm	1077	1791	2.13	2	83	15			
64	Gd	1313	3266	2.20	2	76	22			
66	Dy	1412	2562	2.30	2	66	32			
67	Ho	1474	2695	2.30	2	66	32			
68	Er	1529	2863	2.36	1	63	35	1		
69	Tm	1545	1947	1.96	13	78	9			
70	Yb	819	1194	2.03	3	88	8			
72	Hf	2227	4602	2.89	3	24	51	21	1	
73	Ta	2996	5425	2.93	2	33	38	24	3	
74	W	3410	5660	3.07	2	23	43	26	5	1
77	Ir	2410	4130	2.66	5	37	46	11	1	
78	Pt	1772	3827	2.08	12	69	18	1		
79	Au	1064	2807	2.97	14	75	11			
82	Pb	327	1740	1.64	36	64				
83	Bi	271.3	1560	1.17	83	17				
90	Th	1750	4790	2.88	0	24	64	12		
92	U	1132	3818	3.18	0	12	58	30		

II. SAHA EQUATIONS

The ion charge state distribution of a plasma in equilibrium can be calculated using a set of Saha equations which have the form

$$\frac{n_e\, n_{Q+1}}{n_Q} = \Lambda_B^{-3}\, \frac{2\,\Sigma_{Q+1}(T)}{\Sigma_Q(T)} \exp\left(-\frac{E_Q - \Delta E_Q}{kT}\right) \qquad (1)$$

$$Q = 1, 2, 3, \ldots, Q_{\max}$$

where n_e and n_Q are the density of free electrons and ions of charge state Q, respectively, $Q=0$ for neutral atoms, $Q=1$ for singly ionized ions, etc., with $Q_{\max}$ the maximum charge state abundant in the plasma; $\Sigma_Q(T)$ is the temperature-dependent partition function of ions of charge state Q, k is the Boltzmann constant, T is the temperature,

$$\Lambda_B = h/\left(2\pi\, m_e\, kT\right)^{1/2} \qquad (2)$$

is the thermal De Broglie wavelength, and E_Q is the ionization energy of the Q-fold charged ion. The lowering of the ionization energy, ΔE_Q, reflects the particle interaction or non-ideal nature of the plasma.

A rigorous expression for ΔE_Q can be found in [19] where electron degeneration have been taken into account and the Coulomb interaction is written as a Padé approximation to interpolate between the quantum-corrected Debye law and analytical expressions for the strongly coupled ionic sub-system which is screened by a "liquid" of degenerated electrons; short-range repulsion between shells of bound electrons of different ions is taken into account by a hard-core interaction [20]. In this way, compositions of non-ideal plasmas with densities of heavy particles as high as 10^{29} m^{-3} can be calculated.

For weakly or moderately non-ideal plasmas (i.e., the degeneration of electrons is not considered and quantum mechanical exchange interaction between bound-shell electrons of neighboring ions can be neglected), the lowering of the ionization energies can be described by the relatively simple Debye-Hückel theory [21]

$$\Delta E_Q = \frac{(Q+1)\, e^2}{4\pi\, \varepsilon_o\, (\lambda_D + \Lambda_B/8)} \qquad (3)$$

where

$$\lambda_D = \left[\varepsilon_0\, kT/e^2 \left(n_e + \sum_Q Q^2\, n_Q\right)\right]^{1/2} \qquad (4)$$

is the Debye length, and ε_o is the permittivity of vacuum.

The partition function reflects the structure of the electron shells and is defined by the equation [22]

$$\Sigma_Q(T) = \sum_{s=1}^{s=s_{\max}} g_{Q,s} \exp\left(-\frac{E_{Q,s}}{kT}\right) \qquad (5)$$

where s is the level index ($s=1$ is the ground state, $s_{\max}$ is the highest excited level which is bound), $g_{Q,s}$ and $E_{Q,s}$ are the statistical weight and the energy of level s of an ion with charge state Q, respectively. The statistical weight $g_{Q,s} = 2J_{Q,s} + 1$ can be obtained using the total angular momentum $J_{Q,s}$ given in spectral tables like [23-25]. The system of equations (1)-(5) is completed by the charge-neutrality condition

$$n_e = \sum_Q^{Q_{\max}} Q\, n_Q \qquad (6)$$

The results of the calculations are presented using the following definitions. The percentages of ion charge states are expressed as particle fractions of all ions (not heavy particles, i.e. without neutrals),

$$f_Q = \frac{n_Q}{\sum_{Q'=1}^{Q'_{\max}} n_{Q'}} \cdot 100\% \qquad (7)$$

to allow comparison with experimental results. Additionally, the amount of neutral atoms is given as

$$f_o = \frac{n_o}{\sum_{Q=0}^{Q_{\max}} n_Q} \cdot 100\% \qquad (8)$$

that is the percentage of the total heavy particle density

$$n_h = \sum_{Q=0}^{Q_{\max}} n_Q \qquad (9)$$

The mean ion charge state is defined by

$$\overline{Q} = \sum_{Q=1}^{Q_{max}} Q\, n_Q \Big/ \sum_{Q=1}^{Q_{max}} n_Q \qquad (10)$$

III. THE PERIODIC TABLE OF VACUUM ARC CSD

The CSD of the dense, non-ideal cathode spot plasma is largely determined by pressure ionization. However, this effect becomes less important when the plasma density decreases due to expansion. It was experimentally found that the CSDs do not depend on the distance from the spot center and therefore the plasma is in non-equilibrium [26-29]. Inelastic collisions between heavy particles (ions, atoms) and free electrons are infrequent at large distances ("large" is here a length of order 100 μm or more, [18]). The plasma is not able to relax to its equilibrium state, i.e., the hypothetical equilibrium state changes faster than the plasma can respond and thus the CSD remains almost constant (it is "frozen"). In contrast, the plasma density in the vicinity of the cathode spot is very high, and collisions are sufficiently frequent so as to establish an equilibrium CSD as described by the Saha equations. The transition from equilibrium (dense plasma close to the cathode spot) to non-equilibrium (expanded plasma far from the spot) can be quantified by the Damköhler number which is defined as the ratio of a characteristic flow time and a characteristic time of non-elastic collisions leading to ionization or recombination. Freezing occurs where non-ideal plasma effects play only a minor role for the final CSD. Therefore, the use of the relatively simple Debye-Hückel model is justified for this work.

The system of equations (1) - (6) has been solved numerically for all metallic elements including the semi-metal carbon and the semiconductors Si and Ge. Ionization energies were taken from the latest edition of the Handbook of Physics and Chemistry [30]. In cases where data were missing in [30], theoretical values given by Carlson et al. [31] have been used. The latter data have been obtained by self-consistent-field Hartree-Fock calculations which differ in some cases from the data in the handbook [30] by more than 20%. Table II shows the ionization energies actually used in the present calculations. Temperature-dependent partition functions have been tabulated for 13 cathode elements (C, Al, Ti, Cr, Fe, Co, Ni, Cu, Zn, Zr, Mo, Ag, and Pb) in the handbook by Drawin and Felenbok [22]. Because the ratio of the partition functions were used in the system of Saha equations and not the partition functions themselves, their absolute values are not important for the final results. Moreover, the partition function have only a small effect compared to the exponential dependence on temperature and ionization energy, see equ. (1). Therefore, the use of constant average values (Table III) for all other elements is acceptable.

Table II. Ionization energies (eV) actually used in the calculations [30] [31]

Z	element	E_0 (eV)	E_1 (eV)	E_2 (eV)	E_3 (eV)	E_4 (eV)	E_5 (eV)	E_6 (eV)	E_7 (eV)
3	Li	5.39	75.64	122.4					
4	Be	9.32	18.21	153.9	217.7				
6	C	11.3	24.38	47.89	64.49	392.1	490.0		
11	Na	5.14	47.29	71.62	98.91	138.4	172.2	208.5	264.3
12	Mg	7.65	15.04	80.14	109.3	141.3	186.8	225.0	266.0
13	Al	5.99	18.83	28.45	120.0	153.8	190.5	241.8	284.7
14	Si	8.15	16.35	33.49	45.14	166.8	205.3	246.5	303.5
19	K	4.34	31.63	45.81	60.91	82.66	99.40	117.6	154.9
20	Ca	6.11	11.87	50.91	67.27	84.50	108.8	127.2	147.2
21	Sc	6.56	12.80	24.76	73.49	91.65	110.7	138.0	158.1
22	Ti	6.83	13.76	27.49	43.27	99.30	119.5	140.8	170.4
23	V	6.75	14.66	29.31	46.71	65.28	128.1	150.6	173.4
24	Cr	6.77	16.49	30.96	49.16	69.46	90.63	160.2	184.7
25	Mn	7.43	15.64	33.67	51.20	72.40	95.60	119.2	194.5
26	Fe	7.90	16.19	30.65	54.80	75.00	99.10	125.0	151.1
27	Co	7.88	17.08	33.50	51.30	79.50	102.0	128.9	157.8
28	Ni	7.64	18.17	35.19	54.90	76.06	108.0	133.0	162.0

29	Cu	7.73	20.29	36.84	57.38	79.80	103.0	139.0	166.0
30	Zn	9.39	17.96	39.72	59.40	82.60	108.0	134.0	174.0
31	Ga	6.00	20.51	30.71	61.65	95.94	130.2	164.5	198.8
32	Ge	7.90	15.93	34.22	45.71	93.50	124.5	162.0	199.5
37	Rb	4.18	27.28	40.00	52.60	71.00	84.40	99.20	136.0
38	Sr	5.69	11.03	42.89	57.00	71.60	90.80	106.0	122.3
39	Y	6.22	12.24	20.52	60.60	77.00	93.00	116.0	129.0
40	Zr	6.63	13.13	22.99	34.34	80.35	98.00	117.7	137.4
41	Nb	6.76	14.32	25.04	38.30	50.55	102.1	125.0	141.0
42	Mo	7.09	16.16	27.13	46.40	54.49	68.83	125.7	143.6
43	Tc	7.28	15.26	29.54	42.22	57.87	73.51	90.14	106.1
44	Ru	7.36	16.76	28.47	49.90	66.89	83.51	100.1	116.7
45	Rh	7.46	18.08	31.06	53.52	70.90	88.99	106.7	124.4
46	Pd	8.34	19.43	32.93	60.87	78.25	95.64	113.6	131.4
47	Ag	7.58	21.49	34.83	60.52	80.01	99.50	119.0	139.2
48	Cd	8.99	16.91	37.48	58.26	79.62	101.0	122.3	143.7
49	In	5.79	18.87	28.03	54.33	77.51	100.7	123.9	147.1
50	Sn	7.34	14.63	30.50	40.74	72.28	98.67	123.5	148.4
51	Sb	8.64	16.53	25.30	44.20	56.00	108.0	121.7	148.2
55	Cs	3.89	23.16	35.25	48.09	60.93	75.61	89.02	118.3
56	Ba	5.21	10.00	34.45	48.40	62.35	76.30	92.53	107.1
57	La	5.58	11.06	19.18	49.95	61.60	78.28	93.12	111.2
58	Ce	5.54	10.85	20.20	36.76	65.55	80.06	95.24	110.4
59	Pr	5.46	10.55	21.62	38.98	57.53	82.22	97.20	112.2
60	Nd	5.53	10.73	22.10	40.40	68.53	83.81	99.09	114.4
61	Pm	5.55	10.90	22.30	41.10	69.75	85.32	100.9	116.4
62	Sm	5.64	11.07	23.40	41.40	70.93	86.76	102.6	118.4
63	Eu	5.67	11.24	24.92	24.92	42.70	72.33	88.47	104.6
64	Gd	6.15	12.09	20.63	44.00	71.99	88.91	105.8	122.7
65	Tb	5.86	11.52	21.91	39.79	73.14	90.35	107.6	124.8
66	Dy	5.94	11.67	22.80	41.40	76.28	93.26	110.3	127.2
67	Ho	6.02	11.80	22.84	42.50	77.53	94.79	112.1	129.3
68	Er	6.11	11.93	22.74	42.70	78.76	96.29	113.8	131.4
69	Tm	6.18	12.05	23.68	42.70	79.98	97.77	115.6	133.4
70	Yb	6.25	12.18	25.05	43.56	81.18	99.24	117.3	135.4
71	Lu	5.43	13.90	20.96	45.25	66.80	98.42	117.3	136.2
72	Hf	6.82	14.90	23.30	33.33	67.82	98.23	117.9	137.5
73	Ta	7.89	14.47	23.49	36.32	49.14	92.66	118.7	139.1
74	W	7.98	15.08	25.43	39.29	53.15	67.01	119.7	140.8
75	Re	7.88	15.73	25.89	41.49	56.33	71.17	86.01	142.9
76	Os	8.70	16.34	27.71	42.70	59.29	75.04	90.80	106.5
77	Ir	9.10	16.91	29.50	45.33	61.16	78.70	95.32	111.9
78	Pt	9.00	19.24	35.25	51.27	67.28	83.29	101.0	117.9
79	Au	9.23	20.50	37.37	54.80	70.99	87.81	104.6	123.2
80	Hg	10.4	18.76	34.20	52.93	71.09	89.24	107.4	125.6
81	Tl	6.11	20.43	29.83	50.17	69.70	89.23	108.8	128.3
82	Pb	7.42	15.03	31.94	42.32	68.80	87.98	108.7	129.5
83	Bi	7.29	16.69	26.85	46.06	58.16	85.78	107.7	129.6
84	Po	8.42	17.18	29.01	39.58	61.26	74.08	105.7	128.7
87	Fr	3.61	20.02	31.63	43.25	54.87	71.74	84.94	114.2
88	Ra	5.28	10.15	30.97	43.49	56.02	68.55	87.42	101.6
89	Ac	5.17	12.10	16.93	43.36	56.66	69.95	83.25	104.3
90	Th	6.08	11.50	20.00	28.80	57.22	71.21	85.20	99.18
91	Pa	5.89	11.46	17.75	28.91	46.69	74.36	88.37	102.4
92	U	6.19	11.63	18.09	30.90	49.91	68.91	90.35	104.7
93	Np	6.27	11.80	18.37	32.75	52.83	72.91	92.14	106.7
94	Pu	6.06	11.19	20.70	40.80	60.90	80.40	94.89	109.4
95	Am	5.99	12.15	18.82	36.15	58.14	80.12	95.31	110.4

Table III. Constant partition functions used for most calculations; the data are average values of the data for C, Al, Ti, Cr, Fe, Co, Ni, Cu, Zn, Zr, Mo, Ag, and Pb taken from the handbook by Drawin and Felenbok [22] at the effective freezing parameters for each element.

ion charge state Q	partition function Σ_Q
0	280
1	150
2	45
3	15
4	12
5	6
6	1

The calculations of plasma compositions (i.e., CSDs) were started for the 13 elements with variable, tabulated partition functions. The following scheme was used to calculate the CSD at a preset electron temperature and density: An initial neutral atom density was assumed and the set of Saha equations was solved, resulting in a "temporary" electron density which usually was different from the preset electron density. The assumed neutral density was then varied to minimize the difference between the preset and calculated electron density until a self-consistent CSD was obtained. The calculation was continued with the same temperature at the next preset electron density. The calculation was stopped at high densities when the lowering of the ionization energy approaches the ionization energy. This is the region of strongly non-ideal plasma where the Debye-Hückel theory is not valid anymore. The next step was to compare calculated with experimental CSD data. The experimental mean ion charge state, $\overline{Q}_{exp}$, was taken from Table I, and the mean ion charge state closest to $\overline{Q}_{exp}$ was identified for the given temperature. This closest value was labeled $\overline{Q}_{cal}$, and the CSD associated with $\overline{Q}_{cal}$ was compared with the experimental CSD associated with $\overline{Q}_{exp}$. Usually they didn't match. The whole procedure was repeated for a different preset temperature. It turned out that the calculated CSD becomes broader at higher temperatures for a given $\overline{Q}_{exp}$. This feature allows us to repeat the calculations with higher or lower temperature for too narrow or too broad calculated CSD, respectively, until the calculated and experimental CSDs become similar. There is of course no guarantee that they will indeed become similar because the assumptions underlying the calculations might not be valid. However, the procedure was successful in most cases in the sense that the measured CSDs could be reproduced by the calculations.

As an example for the calculations, Fig. 1 shows the equilibrium plasma composition of a bismuth plasma at three different temperatures (1.6 eV (a), 2.3 eV (b), and 3.1 eV (c)). All results are conveniently presented in the form of a "Periodic Table of Vacuum Arc CSD" (Table IV). Percentages of neutral atoms appear in Table IV but are written in parentheses to distinguish them from ion particle fraction (note the difference in definitions equ. (7) and (8)). The calculated density of neutral atoms is the result of ionization and recombination reaction under equilibrium conditions; it does not include the enhancement due to evaporating macroparticles and evaporation from hot, liquid metal pools of previously active craters.

The close agreement of many experimental CSD (Table I) with the theoretical values (Table IV) justifies the assumptions made: (i) the spot plasma experiences an almost instantaneous transition from equilibrium to non-equilibrium while expanding, and (ii) the plasma parameters at the freezing point fluctuate only marginally allowing determination of an average "effective freezing temperature" and an "effective freezing density" for most elements.

There are two "problematic" groups of cathode elements. One group of elements has the "problem" that their CSD is dominated by only one or two charge states (for instance: Li, C, Zn, Sr, Cd, Sn, Sb, Ba, Pb). This results in a large uncertainty of the calculated effective temperature (± 0.5 eV) and density at freezing ($\pm$ order of magnitude or even more) because the CSDs of these elements are relatively insensitive to variations of temperature and density. This has been marked with "U" (= uncertain) in Table IV.

The other "problematic" group includes Mo, Ag, Hf, Ta, W, and Ir. The experimentally observed CSDs are substantially broader than the calculated (marked with "B" (= broadened CSD) in Table IV). The assumptions are obviously not well justified for these elements.

It is known that the experimental CSDs have been determined by averaging over many individual discharges. The cathode spots are of non-stationary nature, and a CSD measured at a certain instant of time and for an individual pulsed discharge differs from a CSD measured at a different time or discharge even when the macroscopic conditions are kept constant. For

instance, the Figures 4-6 of Ref. [10] show that CSDs scatter when individually measured for a 200 ns window 100 μs after discharge triggering. The scattering of individual CSD suggests that the plasma parameters fluctuate; a well-know phenomena of vacuum arcs. Therefore, it must be expected that experimentally determined, average CSDs are broader than the CSDs calculated with a single "effective temperature" and "effective density" at freezing. The present calculations suggest that this broadening mechanism is particularly pronounced for the "problematic" elements Mo, Ag, Hf, Ta, W, and Ir.

Experiments and calculations show that there exist groups of similar elements. Many features behave periodically and this allows prediction of the CSDs of metals which have so far never been used as vacuum arc cathodes. By comparison with similar elements, effective freezing temperatures and densities have been determined for each "new" element under the conditions of low current and without magnetic fields [32]. Saha calculations have been performed in the same manner as described before (section IV), and the resulting CSD are included in Table IV.

A legitimate question is how reliable these predictions are. The CSD of some elements (Na, K, Rb, Cs, Fr, Ra, Ga) are dominated by a single charge state, almost independent of the freezing parameters; thus it can be assumed that precisely these CSDs will be found in future experiments. The situation is related to the inverse problem of "uncertain" determination of effective freezing parameters from experimentally known CSD (comment "U" in Table IV).

In the other cases, the CSDs depend on the effective freezing parameters, and a relatively large error in the ion percentages is possible (factor two or even more). However, the calculations are qualitatively meaningful because they predict dominant ion charge states and approximate mean charge states. Moreover, the grouping of element properties also allows one to predict that future experimental CSDs of Tc, Ru, Rh, Re, and Os will be broadened comparably to the presented calculated CSDs because all similar elements (Nb, Mo, Hf, Ta, W) show substantial broadening.

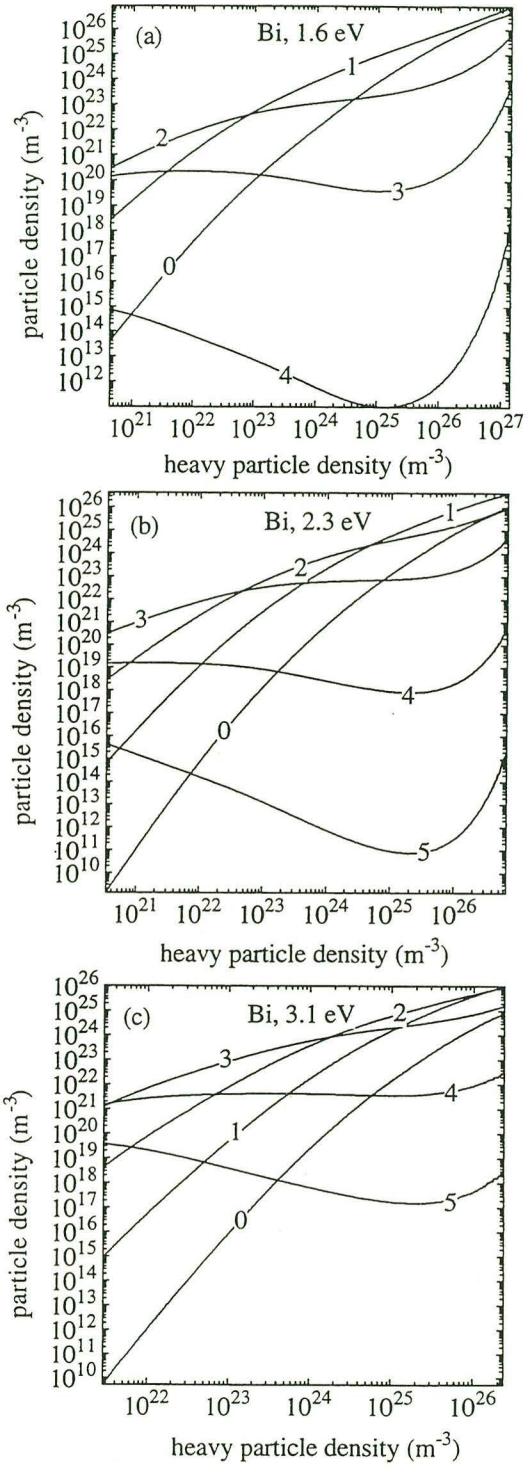

FIG. 1 Example of Saha calculations in Debye-Hückel approximation: equilibrium plasma composition for a bismuth plasma at 1.6 eV (a), 2.3 eV (b), and 3.1 eV (c). The numbers indicate the ion charge state.

Table IV. (next page) **The Periodic Table of Vacuum Arc CSD**. The KEY indicates the order of data; the mean ion charge state is underlined; the particle percentages are defined by equations (7) and (8); the densities and temperature at the CSD freezing point are given in m^{-3} and eV, respectively. Notation: 2.0E24 = 2.0×10^{24}. The symbols of "new" (not yet experimentally investigated) elements are written in *italics*. The last line in each element box shows comments: ! = very good agreement with experimental CSD data; VP = calculation done with **v**ariable **p**artition function (if not stated, the constant partition functions of Table III have been used); B = experimental CSD is substantially **b**roadened; U = **u**ncertain temperature and density at freezing (due to relative insensitivity of CSD on temperature and density); N = "**n**ew" element. The table below givens the grouping of elements (color code).

color code	group of element	typical mean ion charge state
	alkali metals (IA group): Li, Na, K, Rb, Cs, Fr	1.0
	alkaline earth metals (IIA group): Be, Mg, Ca, Sr, Ba, Ra	2.0
	transition metals of the IIIA-VIA group: Al, Ga, In, Tl, Sn, Pb, Sb, Bi, Po	1.2 - 1.6
	transition metals of the IIIB-VIIB group: Sc, Y, Ti, Zr, V, Cr, Mn,	1.8 - 2.2
	ferromagnetic metals of the VIII group: Fe, Co, Ni;	1.7 - 1.8
	refractory and other high melting point and metals (IVB-VIIB and VIII group): Nb, Mo, Tc, Ru, Rh, Hf, Ta, W, Re, Os, Ir,	3.0
	high conductivity metals (IB group): Cu, Ag, Au, including the precious metals of the VIII group; Pd and Pt	1.9 - 2.1
	transition metals of the IIB group: Zn, Cd, Hg	1.3
	semi-metal: C	1.0
	semiconductors: Si and Ge	1.4
	Lanthanides: La, Ce, Pr, Nd, Pm, Sm, Eu, Gd, Tb, Dy, Ho, Er, Tm, Yb, Lu	2.2
	Actinides: Ac, Th, Pa, U, Np, Pu, Am	2.8 - 3.0

KEY

element number, name
(neutral (% of n_h))
onefold (%)
twofold (%)
threefold (%)
fourfold (%)
electron density (m^{-3})
heavy particle density (m^{-3})
temperature (eV)

22 Ti 2.03 — mean ion charge
(0: 4.2E-2)
1: 9.8
2: 78.0
3: 12.3
4: 8.8E-3
n_e= 1.7E25
n_h= 8.2E24
T= 3.2; VP — comment

1 H																2 He
3 Li 1.00 (0: 1.5E-2) 1: 100. 0 2: 2E-13 3: 0 4: 0 n_e= 1.0E23 n_h= 1.0E23 T= 2.0; !, U	4 *Be* 1.30 (0: 1.5) 1: 70.0 2: 30.0 3: 0 4: 0 n_e= 3.1E24 n_h= 2.4E24 T= 2.1; N											5 B	6 C 1.00 (0: 3.52) 1: 99.7 2: 0.30 3: 5.1E-8 4: 0 n_e= 1.6E25 n_h= 1.0E25 T= 2.0; !, U	7 N	8 O	9 F	10 Ne
11 *Na* 1.00 (0: 2.2E-2) 1: 100.0 2: 1.8E-5 3: 0 4: 0 n_e= 1.0E23 n_h= 1.0E23 T= 1.8; N	12 Mg 1.54 (0: 0.82) 1: 46.0 2: 54.0 3: 3.1E-15 4: 0 n_e= 6.0E24 n_h= 3.9E24 T= 2.1; !, U											13 Al 1.73 (0: 0.14) 1: 36.2 2: 54.4 3: 9.5 4: 3.3E-15 n_e= 1.4E25 n_h= 8.2E24 T= 3.1; !,VP	14 Si 1.39 (0: 1.1) 1: 60.8 2: 39.2 3: 6.5E-3 4: 0 n_e= 3.3E24 n_h= 2.4E24 T= 2.0; B	15 P	16 S	17 Cl	18 Ar
19 *K* 1.00 (0: 1.7E-2) 1: 99.9 2: 0.1 3: 3.5E-9 4: 0 n_e= 1.0E23 n_h= 1.0E23 T= 1.7; N	20 Ca 1.93 (0: 2.6E-2) 1: 7.0 2: 93.0 3: 3.2E-5 4: 0 n_e= 2.9E24 n_h= 1.5E24 T= 2.2	21 Sc 1.79 (0: 0.47) 1: 23.6 2: 73.7 3: 2.7 4: 5.4E-10 n_e= 2.4E25 n_h=1.3E25 T= 2.4	22 Ti 2.03 (0: 4.2E-2) 1: 9.8 2: 78.0 3: 12.3 4: 8.8E-3 n_e= 1.7E25 n_h= 8.2E24 T= 3.2; VP	23 V 2.14 (0: 0.37) 1: 5.5 2: 75.0 3: 19.5 4: 3.8E-2 n_e= 1.7E25 n_h= 8.1E24 T= 3.4	24 Cr 2.09 (0: 3.7E-2) 1: 9.6 2: 71.8 3: 18.6 4: 5.6E-2 n_e= 2.0E25 n_h= 9.6E24 T= 3.4; VP	25 Mn 1.52 (0: 1.3) 1: 48.0 2: 51.9 3: 0.1 4: 8.7E-7 n_e= 4.5E25 n_h= 3.0E25 T= 2.6	26 Fe 1.82 (0: 0.37) 1: 24.1 2: 69.7 3: 6.2 4: 3.2E-3 n_e= 4.4E25 n_h= 2.4E25 T=3.4; !, VP	27 Co 1.73 (0: 0.78) 1: 27.9 2: 71.7 3: 0.44 4: 4.7E-5 n_e= 2.5E25 n_h= 1.4E25 T= 3.0; VP,B	28 Ni 1.76 (0: 0.59) 1: 24.5 2: 74.7 3: 0.77 4: 3.5E-5 n_e= 1.5E25 n_h= 8.8E24 T= 3.0; VP,B	29 Cu 2.06 (0: 3.0E-2) 1: 10.7 2: 72.1 3: 17.1 4: 1.4E-2 n_e= 4.8E24 n_h= 2.3E24 T= 3.5; VP,B	30 Zn 1.20 (0: 8.3) 1: 80.0 2: 20.0 3: 3E-4 4: 0 n_e= 5.9E24 n_h= 5.4E24 T=2.0; !,VP,U	31 *Ga* 1.06 (0: 0.67) 1: 93.7 2: 6.3 3: 3.5E-3 4: 0 n_e= 3.9E24 n_h= 3.7E24 T= 2.0; N	32 Ge 1.40 (0: 1.8) 1: 59.6 2: 40.4 3: 4.0E-5 4: 3.8E-9 n_e= 4.0E24 n_h= 2.9E24 T= 2.0; !, U	33 As	34 Se	35 Br	36 Kr
37 *Rb* 1.00 (0: 2.0E-2) 1: 99.8 2: 0.2 3: 9.7E-8 4: 0 5: 0 6: 0 n_e= 1.0E23 n_h= 1.0E23 T= 1.6; N	38 Sr 1.98 (0: 3.1E-3) 1: 2.0 2: 98.0 3:1.8E-3 4: 0 5: 0 6: 0 n_e= 2.3E24 n_h=1.2E24 T= 2.5; !,U	39 Y 2.28 (0: 0.023) 1: 5.1 2: 62.0 3: 32.9 4: 2.9E-6 5: 0 6: 0 n_e= 5.2E24 n_h= 2.3E24 T= 2.4; !	40 Zr 2.58 (0: 6.1E-3) 1: 1.5 2: 46.3 3: 45.0 4: 7.2 5: 1.7E-3 6: 0 n_e= 2.2E25 n_h= 8.4E24 T= 3.7; !,VP	41 Nb 3.00 (0: 1.9E-3) 1: 0.6 2: 19.4 3: 59.9 4: 19.8 5: 0.24 6: 1.8E-9 n_e= 1.9E25 n_h= 6.2E24 T= 4.0; B	42 Mo 3.06 (0: 4.1E-4) 1: 0.2 2: 7.7 3: 78.4 4: 13.6 5: 8.4E-2 6: 3.4E-5 n_e=1.8E25 n_h= 6.0E24 T= 4.5; VP,B	43 *Tc* 3.00 (0: 6.0E-4) 1: 0.35 2: 19.6 3: 60.0 4: 19.9 5: 0.13 6: 8.1E-6 n_e= 1.4E25 n_h= 4.6E24 T= 4.5; N	44 *Ru* 2.90 (0: 6.1E-4) 1: 0.36 2: 16.9 3: 74.9 4: 7.8 5: 1.3E-2 6: 2.2E-7 n_e= 1.2E25 n_h= 4.0E24 T= 4.5; N	45 *Rh* 2.77 (0: 9.5E-3) 1: 0.64 2: 25.3 3: 70.4 4: 3.6 5: 2.8E-3 6: 1.4E-8 n_e= 1.0E25 n_h= 3.6E24 T= 4.5; B	46 Pd 1.88 (0: 0.16) 1: 19.7 2: 72.3 3: 7.8 4: 8.5E-4 5: 5.3E-10 6: 0 n_e= 2.0E25 n_h= 1.0E25 T= 3.5; B	47 Ag 2.14 (0: 5.7E-2) 1: 3.8 2: 78.5 3: 17.6 4: 0.012 5: 6.6E-8 6: 0 n_e= 2.8E25 n_h= 1.3E25 T= 4.0; VP,B	48 Cd 1.32 (0: 2.3) 1: 68.0 2: 32.0 3: 1.2E-3 4: 0 5: 0 6: 0 n_e= 6.0E24 n_h= 4.6E24 T= 2.1; !,U	49 In 1.34 (0: 2.0) 1: 66.0 2: 34.0 3: 1.3E-3 4: 0 5: 0 6: 0 n_e= 5.3E24 n_h= 4.0E24 T= 2.1; !, U	50 Sn 1.53 (0: 1.0) 1: 47.0 2: 53.0 3: 4.6E-2 4: 0 5: 0 6: 0 n_e= 8.3E24 n_h= 5.4E24 T= 2.1; !, U	51 Sb 1.01 (0: 26.9) 1: 99.2 2: 0.8 3: 1.47E-5 4: 0 5: 0 6: 0 n_e= 6.3E24 n_h= 8.6E23 T= 1.4; !, U	52 Te	53 I	54 Xe
55 *Cs* 1.01 (0: 2.1E-2) 1: 99.2 2: 0.7 3: 1.8E-6 4: 0 5: 0 6: 0 n_e= 1.0E23 n_h= 1.0E23 T= 1.5; N	56 Ba 2.00 (0: 2.1E-3) 1: 0.54 2: 98.9 3: 0.52 4: 1.6E-5 5: 0 6: 0 n_e= 5.1E23 n_h= 2.5E23 T= 2.3; !, U	57 La* 2.22 (0: 1.1E-4) 1: 0.88 2: 76.2 3: 22.9 4: 5.0E-12 5: 0 6: 0 n_e= 1.4E22 n_h= 6.1E21 T= 1.4; !, U	72 Hf 2.89 (0: 0.011) 1: 2.0 2: 26.6 3: 51.7 4: 19.7 5: 4.2E-4 6: 0 n_e= 2.5E25 n_h= 8.7E24 T= 3.6; B	73 Ta 2.93 (0: 4.7E-3) 1: 1.0 2: 21.7 3: 61.1 4: 16.1 5: 0.11 6: 2.2E-9 n_e= 1.7E25 n_h= 5.9E24 T= 3.7; B	74 W 3.07 (0: 3.0E-3) 1: 0.61 2: 16.8 3: 58.1 4: 24.2 5: 0.32 6: 6.8E-5 n_e= 2.8E25 n_h= 9.0E24 T= 4.3; B	75 *Re* 3.05 (0: 1.4E-3) 1: 0.44 2: 15.0 3: 63.7 4: 20.7 5: 0.16 6: 1.6E-5 n_e= 1.8E25 n_h= 5.8E24 T= 4.3; N	76 *Os* 2.95 (0: 2.2E-3) 1: 0.63 2: 20.6 3: 62.2 4: 16.5 5: 6.8E-2 6: 2.9E-6 n_e= 1.6E25 n_h= 5.3E24 T= 4.3; N	77 Ir 2.66 (0: 7.0E-3) 1: 1.6 2: 36.4 3: 56.2 4: 5.8 5: 1.0E-2 6: 1.1E-7 n_e= 1.7E25 n_h= 6.4E24 T= 4.2; B	78 Pt 2.08 (0: 5.0E-2) 1: 7.8 2: 76.4 3: 15.6 4: 0.17 5: 2.5E-5 6: 0 n_e= 2.1E25 n_h= 1.0E25 T= 4.0; B	79 Au 1.97 (0: 8.2E-2) 1: 12.5 2: 77.8 3: 9.6 4: 5.1E-2 5: 3.0E-6 6: 0 n_e= 2.0E25 n_h= 1.0E25 T= 4.0; !	80 *Hg* 1.32 (0: 2.7) 1: 68.5 2: 31.5 3: 2.4E-2 4: 1.6E-8 5: 0 6: 0 n_e= 6.0E24 n_h= 4.7E24 T= 2.3; N	81 *Tl* 1.60 (0: 0.28) 1: 41.6 2: 56.8 3: 1.6 4: 4.9E-4 5: 0 6: 0 n_e= 7.5E23 n_h= 4.7E23 T= 2.3; N	82 Pb 1.64 (0: 0.51) 1: 36.3 2: 63.5 3: 0.22 4: 1.3E-6 5: 0 6: 0 n_e= 1.6E24 n_h= 9.9E23 T= 2.0; !, U	83 Bi 1.17 (0: 1.4) 1: 83.0 2: 16.9 3: 3.4E-2 4: 4.3E-7 5: 0 6: 0 n_e= 3.1E24 n_h= 2.7E24 T= 1.8; !, U	84 *Po* 1.20 (0: 1.6) 1: 79.8 2: 20.2 3: 9.2E-3 4: 0 5: 0 6: 0 n_e= 1.7E24 n_h= 1.4E24 T= 1.8; N	85 At	86 Rn
87 *Fr* 1.05 (0: 1.7E-2) 1: 94.5 2: 5.5 3: 2.2E-4 4: 0 n_e= 9.5E22 n_h= 1.0E23 T= 1.5; N	88 *Ra* 1.99 (0: 1.4E-3) 1: 1.5 2: 98.1 3: 0.4 4: 1.0E-5 n_e= 8.2E23 n_h= 4.1E23 T= 2.1; N	89 *Ac*** 2.87 (0: 1.7E-4) 1: 0.27 2: 12.4 3: 87.3 4: 1.67 n_e= 8.6E23 n_h= 3.0E23 T= 2.3; N	104 Rf	105 Ha	106 Sg	107 Ns	108 Hs	109 Mt														

* Lanthanides	58 Ce 2.11 (0: 2.0E-3) 1: 2.5 2: 83.8 3: 13.7 4: 3.4E-4 n_e= 2.4E23 n_h= 1.1E23 T= 1.7; !	59 Pr 2.25 (0: 1.2E-2) 1: 3.0 2: 69.6 3: 27.4 4: 3.2E-2 n_e= 7.2E24 n_h= 3.2E24 T= 2.5; !	60 Nd 2.17 (0: 3.5E-5) 1: 0.36 2: 82.1 3: 17.5 4: 1.0E-5 n_e= 2.1E22 n_h= 9.4E21 T= 1.6; !	61 *Pm* 2.15 (0: 2.74E-4) 1: 0.87 2: 82.8 3: 16.3 4: 2.36E-4 n_e= 1.2E23 n_h= 5.5E22 T= 1.8; N	62 Sm 2.13 (0: 2.8E-3) 1: 2.1 2: 82.9 3: 15.0 4: 2.1E-3 n_e= 1.2E24 n_h= 5.8E23 T= 2.2; !	63 *Eu* 2.10 (0: 1.5E-4) 1: 0.65 2: 88.9 3: 10.5 4: 2.7E-4 n_e= 1.0E23 n_h= 4.9E22 T= 1.9; N	64 Gd 2.20 (0: 1.0E-3) 1: 2.1 2:76.4 3: 21.5 4: 1.6E-4 n_e= 9.9E22 n_h= 4.5E22 T= 1.7	65 *Tb* 2.25 (0: 1.56E-3) 1: 1.6 2: 71.5 3: 26.8 4: 5.3E-3 n_e= 6.3E23 n_h= 2.8E23 T= 2.1; N	66 Dy 2.30 (0: 2.5E-3) 1: 1.7 2: 66.5 3: 31.8 4: 1.8E-2 n_e= 1.7E24 n_h=7.4E23 T= 2.4; !	67 Ho 2.30 (0: 2.6E-3) 1: 1.8 2: 66.4 3: 31.8 4: 1.2E-2 n_e= 1.7E24 n_h= 7.2E23 T= 2.4; !	68 Er 2.36 (0: 1.6E-4) 1: 0.57 2: 63.0 3: 36.4 4: 2.5E-3 n_e= 1.3E23 n_h= 5.5E22 T= 2.0	69 Tm 1.96 (0: 0.19) 1: 12.9 2: 77.9 3: 9.0 4: 2.5E-3 n_e= 2.8E25 n_h= 1.4E25 T= 2.6; !	70 Yb 2.03 (0: 7.6E-3) 1: 4.0 2: 88.9 3: 7.1 4: 3.4E-4 n_e= 1.3E24 n_h= 6.6E23 T= 2.2; !	71 *Lu* 2.00 (0: 0.11) 1: 17.2 2: 64.1 3: 18.2 4: 6.6e-4 n_e= 1.0E25 n_h= 5.1E24 T= 2.0; N
** Actinides	90 Th 2.88 (0: 2.5E-7) 1: 0.3 2: 23.4 3: 64. 3 4: 12.0 5: 1.1E-5 6: 0 n_e= 8.7E23 n_h= 3.0E23 T= 2.4; !	91 *Pa* 3.14 (0: 1.2E-3) 1: 0.34 2: 11.0 3: 61.6 4: 25.6 5: 2.3E-2 6: 8.4E-10 n_e= 1.0E25 n_h= 3.3E24 T= 3.0; N	92 U 3.18 (0: 1.95E-3) 1: 0.35 2: 9.7 3: 60.9 4: 29.0 5: 0.04 6: 8.9E-7 n_e= 2.5E25 n_h= 7.9E24 T= 3.4	93 *Np* 2.93 (0: 1.6E-3) 1: 0.48 2: 15.2 3: 75.1 4: 9.2 5: 1.1E-3 6: 6.6E-11 n_e= 8.9E24 n_h= 3.0E24 T= 3.0; N	94 *Pu* 2.68 (0: 2.7E-3) 1: 0.8 2: 31.0 3: 67.6 4: 0.54 5: 4.1E-6 6: 0 n_e= 9.2E24 n_h= 3.4E24 T= 3.0; N	95 *Am* 2.83 (0: 2.05E-3) 1: 0.66 2: 18.5 3: 77.8 4: 3.0 5: 6.0E-5 6: 0 n_e= 9.0E24 n_h= 3.2E24 T= 3.0; N							

ACKNOWLEDGMENTS

I would like to thank Tom Schülke for his help in the numerical solution of the Saha equations. I also would like to acknowledge stimulating discussions with Andreas Förster, Simone Anders, Ian Brown, Burkhard Jüttner, Efim Oks, and Georgi Yushkov. This work was supported by the U.S. Department of Energy, Division of Advanced Energy Projects, under contract No. DE-AC03-76SF00098.

REFERENCES

[1] J. M. Lafferty, *Vacuum Arcs – Theory and Applications*. New York: Wiley, 1980.

[2] R. L. Boxman, D. M. Sanders, and P. J. Martin, *Handbook of Vacuum Arc Science and Technology*. Park Ridge: Noyes Publications, 1995.

[3] B. Jüttner, "Characterization of the cathode spot," *IEEE Trans. Plasma Sci.*, vol. PS-15, pp. 474-480, 1987.

[4] G. A. Mesyats and D. I. Proskurovsky, *Pulsed Electrical Discharge in Vacuum*. Berlin: Springer-Verlag, 1989.

[5] V. M. Lunev, V. G. Padalka, and V. M. Khoroshikh, "Plasma properties of a metal vacuum arc," *Sov. Phys. Tech. Phys.*, vol. 22, pp. 858-861, 1977.

[6] W. D. Davis and H. C. Miller, "Amalysis of the electrode products emitted by dc arcs in a vacuum ambient," *J. Appl. Phys.*, vol. 40, pp. 2212-2221, 1969.

[7] A. A. Plyutto, V. N. Ryzhkov, and A. T. Kapin, "High speed plasma streams in vacuum arcs," *Sov. Phys. JETP*, vol. 20, pp. 328-337, 1965.

[8] I. G. Brown, B. Feinberg, and J. E. Galvin, "Multiply stripped ion generation in the metal vapor vacuum arc," *J. Appl. Phys.*, vol. 63, pp. 4889 - 4898, 1988.

[9] I. G. Brown and X. Godechot, "Vacuum arc ion charge-state distributions," *IEEE Trans. Plasma Sci.*, vol. PS-19, pp. 713-717, 1991.

[10] A. Anders, S. Anders, B. Jüttner, and I. G. Brown, "Time dependence of vacuum arc parameters," *IEEE Trans. Plasma Sci.*, vol. PS-21, pp. 305-311, 1993.

[11] E. Oks, I. G. Brown, M. R. Dickinson, R. A. MacGill, P. Spädtke, H. Emig, and B. H. Wolf, "Elevated ion charge states in vacuum arc plasmas in a magnetic field," *Appl. Phys. Lett.*, vol. 67, pp. 200-202, 1995.

[12] F. J. Paoloni and I. G. Brown, "Some observations of the effect of magnetic field and arc current on the vacuum arc charge state distribution," *Rev Sci. Instrum.*, vol. 66, pp. 3855-3858, 1995.

[13] I. G. Brown, "Vacuum arc ion sources," *Rev. Sci. Instrum.*, vol. 65, pp. 3061-3081, 1994.

[14] A. Anders, I. Brown, M. Dickinson, and R. MacGill, "High ion charge states in a high-current, short-pulse vacuum arc ion source," *Rev. Sci. Instrum.*, vol. 67, pp. 1202-1204, 1996.

[15] J. E. Galvin, I. G. Brown, and R. A. MacGill, "Charge state distribution studies of the metal vapor vacuum arc ion source," *Rev. Sci. Instrum.*, vol. 61, pp. 583-585, 1990.

[16] I. G. Brown, J. E. Galvin, R. A. MacGill, and M. W. West, "Multiply charged metal ion beams," *Nucl. Instrum Meth. Phys. Res. B*, vol. 43, pp. 455-458, 1989.

[17] E. M. Oks, A. Anders, I. G. Brown, M. R. Dickinson, and R. A. MacGill, "Ion charge state distributions in high current vacuum arc plasma in a magnetic field," *IEEE Trans. Plasma Sci.*, pp. in print (June 1996).

[18] A. Anders, S. Anders, and E. Hantzsche, "Validity conditions for complete and partial local thermodynamic equilibrium of non-hydrogenic level systems and their application to copper vapor arcs in vacuum," *IEEE Trans. Plasma Sci.*, vol. 17, pp. 653-656, 1989.

[19] A. Anders, S. Anders, A. Förster, and I. G. Brown, "Pressure ionization: its role in metal vapor vacuum arc plasmas and ion sources," *Plasma Sources Sci. Technol.*, vol. 1, pp. 263-270, 1992.

[20] W. Ebeling, A. Förster, V. E. Fortov, V. K. Gryaznov, and A. Y. Polishchuk, *Thermophysical Properties of Hot Dense Plasma*, vol. 25. Stuttgart and Leipzig: Teubner Verlagsgesellschaft, 1991.

[21] W. Ebeling, W.-D. Kremp, and D. Kraeft, *Theory of Bound States and Ionization Equilibrium in Plasmas and Solids*. Berlin: Akademie-Verlag, 1976.

[22] H.-W. Drawin and P. Felenbok, *Data for Plasmas in Local Thermodynamic Equilibrium*. Paris: Gauthier-Villars, 1965.

[23] C. E. Moore, *NBS Circular no. 467: Atomic Energy Levels*, vol. I, II, III.

Washington: Nat. Bur. Standards, 1949, 1952, 1958.
[24] S. Bashkin and J. O. Stoner, *Atomic Energy-Level and Grotrian Diagrams, vol. II, Sulfur I - Titanium XXII.* Amsterdam: North-Holland Publ. Comp, 1978.
[25] C. E. Moore, *Selected Tables of Atomic Spectra, A: Atomic Energy Levels CI-CVI*, vol. 3, Sec. 3. Washington: Nat. Bur. Standards, 1970.
[26] C. Wieckert, "A multicomponent theory of the cathodic plasma jet in vacuum arcs," *Contrib. Plasma Phys.*, vol. 27, pp. 309-330, 1987.
[27] S. Anders and A. Anders, "Frozen state of ionization in a cathodic plasma jet of a vacuum arc," *J. Phys. D: Appl. Phys.*, vol. 21, pp. 213-215, 1988.
[28] S. Anders and A. Anders, "Effects of non-ideally and non-equilibrium in the cathode spot plasma of vacuum arcs," *Contrib. Plasma Phys.*, vol. 29, pp. 537-543, 1989.
[29] N. B. Volkov and A. Z. Nemirovsky, "The ionic composition of the non-ideal plasma produced by a metallic sphere isothermally expanding into vacuum," *J. Phys. D: Appl. Phys.*, vol. 24, pp. 693-701, 1991.
[30] D. R. Lide and H. P. R. Frederikse, *Handbook of Physics and Chemistry*, 76 ed. Boca Raton, New York: CRC Press, 1995.
[31] T. A. Carlson, C. W. Nestor, N. Wasserman, and J. D. McDowell, "Ionization Potentials," *Atomic Data*, vol. 2, pp. 63-98, 1970.
[32] A. Anders and T. Schülke, "Predicting ion charge states of vacuum arc plasmas," presented at XVIIth Int. Symp. Discharges and Electrical Insulation in Vacuum, Berkeley, 1996.

Ernest Orlando Lawrence Berkeley National Laboratory
One Cyclotron Road | Berkeley, California 94720

Prepared for the U.S. Department of Energy under Contract No. DE-AC03-76SF00098